

# 6-channel optical demultiplexer based on photonic crystal

A. MOTIE DIZAJI<sup>1</sup>, S. MASOUMI<sup>2,\*</sup>, J. BEIZA<sup>1</sup>, L. MOHAMMADIAN<sup>1</sup>

<sup>1</sup>Department of Electrical Engineering, Shabestar Branch, Islamic Azad university, Shabestar, Iran

<sup>2</sup>Department of Electrical Engineering, Tasouj Branch, Islamic Azad university, Tasouj, Iran

This study has proposed a 6-channel wavelength division demultiplexer based on photonic crystal ring resonators suitable for Wavelength Division Multiplexing (WDM) applications. For this purpose, a demultiplexer of six resonance rings with geometrical parameters has been used with a square grid of two-dimensional photonic crystal structure consisting of dielectric rods as the basic structure for designing a demultiplexer that has two photonic band gap (PBG) regions. The first band gap covers optical communication wavelengths. The minimum transmission efficiency of more than 95% and the average channel spacing of 0.98 nm have been obtained for the designed demultiplexer.

(Received February 11, 2024; accepted July 30, 2024)

**Keywords:** Photonic crystals, Demultiplexer, Resonator

## 1. Introduction

Nowadays, the use of all-optical devices has become inevitable in most fields of electronics and telecommunications. With the development of high-speed telecommunications, there is a growing demand for faster data transmission and processing, as well as for technology that integrates devices. Scientists in this field are considering replacing electronic integrated circuits with optical integrated circuits. This shift is driven by the limitations of electronic integrated circuits, such as slower processing speeds, larger sizes, and the challenges associated with increasing working frequencies. In optical integrated circuits, photons are used as data carriers, offering significant advantages over traditional electronic circuits.

It is of particular importance to design optical devices in small sizes for optical integrated circuits. However, designing optical devices with very small sizes is always a challenge due to the weak confinement of light in small spaces. Photonic crystals have solved this problem due to their periodic nature. It is possible to design different devices with different applications in the field of optical communication and optoelectronics according to optical integrated circuits by using these structures. These devices can be used to design optical filters [1-4], optical demultiplexers [5-7] all-optical switches [8-9], and other optical devices with telecommunication applications [1]. The use of WDM (Wavelength Division Multiplexing) technology makes it possible to use an optical fiber to transmit several optical channels with different wavelengths that operate independently of each other [10-12]. It should be possible to separate the different channels in the optical receiver after sending the optical information. This shows the importance of using optical demultiplexer [13-15]. In fact, WDM combines several optical signals, amplifies them, and sends them as a set, which increases the capacity. The distance between the wavelengths used to transmit information should be reduced to maximize the use

of fiber capacity in this method to send more information on the fiber.

Currently, the WDM system is divided into three categories: WDM, DWDM, and CWDM in the wavelength pattern in this system, light waves are divided into three regions: ultraviolet, visible, and infrared. However, for telecommunication applications, the infrared region is divided into smaller regions called the first to the fourth window. The central wavelength of the first to fourth window is 810, 1310, and 1550 nm, respectively, which are known as fiber windows. The third window is known as the C band, the most important of which is its use in telecommunication networks. Its wavelength range is 1530 to 1570 nm and has the lowest losses in telecommunication systems.

RSoft Photonics CAD software is considered one of the most powerful commercial tools for designing and analyzing optical devices. In this article, it is used to simulate a demultiplexer based on photonic crystals. This software allows for numerical calculations related to the photonic crystals' forbidden band and can calculate the frequency response of various structures. Additionally, it provides a way to visualize the propagation of different light waves within the structure.

The performance of the demultiplexer is evaluated based on its ability to effectively separate the input and output channels [16]. In this study, we examine several different demultiplexer designs, focusing on the spacing of the channels obtained.

Talebzadeh et al. [16] designed 6 and 8-channel demultiplexers based on two-dimensional photonic crystals. Silicon and carbon rods with different radii were used in ring resonators, both in the main rings and the base structures. In these designs, the channel spacing was 1.46 nm for the 6-channel demultiplexer and 1.15 nm for the 8-channel demultiplexer.

Talebzadeh et al. [17] designed a 4-channel optical demultiplexer using a standing-wave (or linear) cavity. The structure achieved an average Q factor of 4107, a

transmission efficiency of 93%, and a crosstalk of approximately -27 dB, with a channel spacing of about 2 nm. Initially, an optical filter was designed using a linear resonator, yielding favorable results. The study then examined how changes in the radius of the dielectric rods in the resonator affected the filter's suitability for use in a demultiplexer. By placing several resonators with varying inner rod radii adjacent to one another and confirming the effectiveness of the filter, a demultiplexer was successfully designed.

Mehdizadeh et al. [18] developed an optical demultiplexer using 8 linear resonators, capable of separating wavelengths between 1536 nm and 1551 nm. The photonic band-gap of the structure spans from 1390 nm to 2035 nm, encompassing the wavelength range targeted by the demultiplexer. The design achieved an inter-channel spacing of 2.1 nm.

Talebzadeh et al. [19] designed and simulated an 8-channel optical demultiplexer using resonant cavities. The structure features an inter-channel spacing of 1.75 nm, a bandwidth of approximately 1.5 nm, a Q factor of about 4860, and a transmission factor exceeding 90%. Additionally, the average inter-channel crosstalk level is around -18 dB. The design incorporates resonator cavities, with adjustments made to the radius of the rods' point defects within the resonator to facilitate wavelength separation. The radius of these rods increases progressively in the demultiplexer structure.

## 2. Theory of ring resonators and demultiplexer design

### 2.1. Theory of ring resonators

A ring resonator is composed of an optical waveguide which loops back on itself, such that resonance occurs only if the optical path length of the resonator matches an exact integer multiple of the wavelength. Specifically, when the electromagnetic waves traveling in the loop pick up a phase shift equal to an integer multiple of  $2\pi$ , the waves interfere constructively to create a resonant cavity. Thus, ring resonators can support multiple resonances but they are not deemed functional as long as there are no coupling to the outside world. Co-directional coupling between the ring and an adjacent waveguide is recognized as the most common coupling mechanism [20, 21].

A bus waveguide with a single ring resonator will display dips in its transmission spectrum around the resonance frequencies of the ring. Thanks to this configuration, the ring resonator acts as a spectral filter, which makes it a perfect choice for numerous optical communication applications, particularly in wavelength-division multiplexing (WDM) [19, 20].

Fig 1 depicts a straightforward model of a basic add-drop ring resonator configuration, which includes an input, an output waveguide, and a ring resonator with a radius  $r$ .

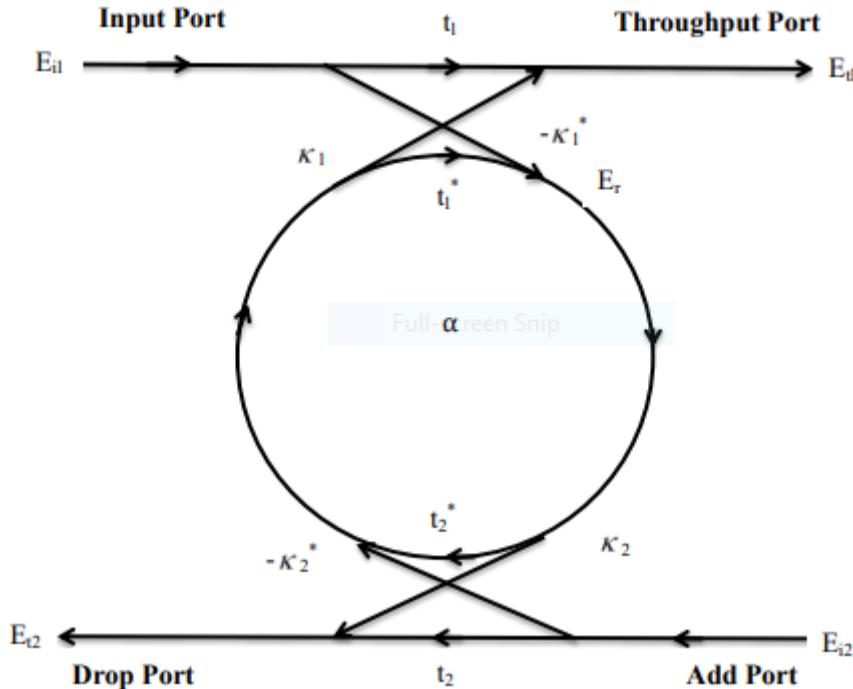


Fig. 1. Model of basic add-drop single resonator filter

The operational power mode amplitude in the first waveguide is given by the following equation [20, 21]:

$$E_{t1} = \frac{t1 - t2^* \alpha e^{j\theta}}{1 - t1^* t2^* \alpha e^{j\theta}} \quad (1)$$

where  $\alpha$  denotes the ring loss coefficient,  $\theta$  denotes phase shift given by  $\theta = \omega L/c$  where  $L$  represents the circumference of the ring given by  $L = 2\pi r$  signifies the radius of the ring from the center of the ring to the center of

the waveguide,  $c$  is the phase velocity of the ring ( $c = c_0/n_{eff}$ ) and  $\omega = kc_0$  denotes the angular frequency with  $c_0$  signifying the speed of light in a vacuum.

The vacuum wave number  $k$  corresponds to the wavelength  $\lambda$  by  $k = 2\pi/\lambda$ . The coupler parameters  $t$  and  $k$  depend on the specific coupling mechanism used. The asterisk symbol indicates the complex conjugate of  $t$  and  $k$ , respectively. The dropped mode amplitude in the second waveguide ( $E_{t2}$ ) is given by the following equation [20, 21]:

$$E_{t2} = \frac{-k1^*k2\alpha_{1/2}e^{j\theta_{1/2}}}{1 - t1^*t2^*\alpha e^{j\theta}} \quad (2)$$

where  $\alpha_{1/2}$  and  $\theta_{1/2}$  denote half round-trip loss and phase, respectively. At resonance conditions, the output intensity from the drop port is given by the following equation [20, 21]:

$$P_{t2-Resonance} = |E_{t2-Resonance}|^2 = \frac{(1 - |t1|^2) \cdot (1 - |t2|^2) \cdot \alpha}{(1 - \alpha|t1t2|^2)^2} \quad (3)$$

The through port mode amplitude  $E$  will be zero at resonance for identical symmetrical couplers ( $t1 = t2$ ), when  $\alpha = 1$  (zero loss). This means that on resonance, all input optical power will be coupled to resonator and could be extracted by drop port [19].

The resonance wavelength of ring resonators can be calculated using the following equation [21]:

$$\lambda_{res} = \frac{n_{eff}L}{m} \quad (4)$$

where  $m$  denotes the integer mode number ( $m = 1, 2, 3$ ) and  $n_{eff}$  signifies the effective refractive index of the ring resonator.

## 2.2. Demultiplexer design

Numerical simulation of Plane Wave Expansion (PWE) and Finite-Difference Time-Domain (FDTD) have

been used to analyze the behavior and extract the characteristics of this device in photonic crystals. RSoft Photonics CAD software package has been used for simulation calculations. This software package is based on BandSOLVE and FullWAVE software.

In the design of the current demultiplexer, compared to the previous demultiplexer, we faced a major challenge, which was the possibility of reducing the space between channels without losing an appreciable transmission power range. One of the effective factors in reducing the space between channels is the arrangement of the rods inside the ring resonators, in this design we obtained the structure by creating diversity in the resonator, in which the space between the channels compared to 6-channel and multi-channel demultiplexers has been improved significantly [16-19].

The designed 6-channel optical demultiplexer is suitable for WDM applications. The wavelength selection mechanism in this work is based on ring resonator structures, we present a device using 6 resonator rings with different core sizes that is able to separate 6 optical channels in the optical communication window. In the designed multiplier valley, the average distance is less than 0.98 nm and the average transmission efficiency for the channels is more than 98%.

In this study, we used a 2D square-lattice PhC consisting of dielectric rods. The number of dielectric rods in the X and Z directions ( $N_x$  and  $N_z$  respectively) is 75 and 53. The lattice constant is 641 nm and the pore radius is 128 nm. The effective refractive index of the ground dielectric is 3.87 in Si/C rods. Extracting the bond structure and finding the (Pare Bird Grod) PBG (Photonic Band Gap) is the first step in designing and analyzing the base structure of PhC. Currently, numerical methods are the best method to extract PhC properties and investigate the behavior of electromagnetic waves in periodic structures such as PhCs. Plane-wave expansion (PWE) is one of the most common numerical methods to calculate the PBG of these structures. The high speed of calculations is its main advantage, but its main drawback is the limitation in calculating the stationary state. We used BandSolve to perform PWE calculations and extract the band structure and PBG of the proposed structure. The simulated dispersion curve is shown in Fig. 2.

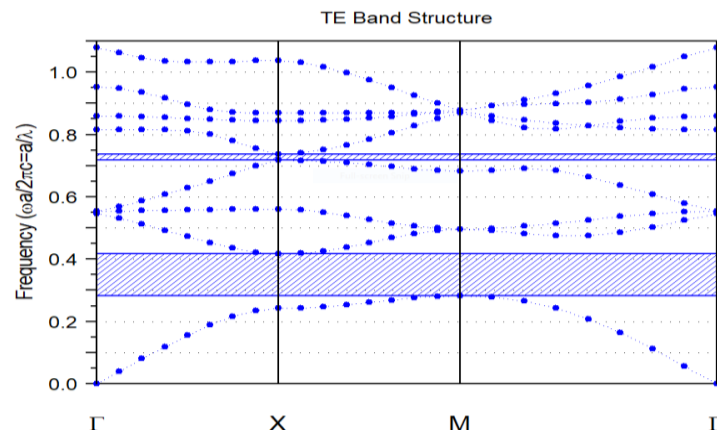


Fig. 2. Band structure of basic PhC structure (The reader is referred to the web version of this article for interpretation of references to color in the text) (color online)

Two PBGs are obtained in TM mode (blue color regions) and no PBG in TE mode (red color regions). The first PBG is between 0.28\_0/98 considering  $a=700\text{nm}$  the PBG will be 1520\_2289nm.

A six-channel optical demultiplexer based on photonic crystal ring resonators is designed and proposed in this study.

The use of ring resonators is to design optical devices based on photonic crystals. In order to create this type of resonator, we take a number of photonic crystal rods to the point where the amount of created defects takes on a ring

state. One of the advantages of this type of resonator compared to other types is the high flexibility of these structures, which justifies their use in designing optical devices based on photonic crystals. The high flexibility of these structures is due to various reasons, among which we can mention the existence of scattering rods, coupling rods, inner rods, and PCRR [7].

The proposed demultiplexer consists of six main parts, one input waveguide, 6 output waveguides, and 6 resonance loops. The proposed demultiplexer is shown in Fig. 3.

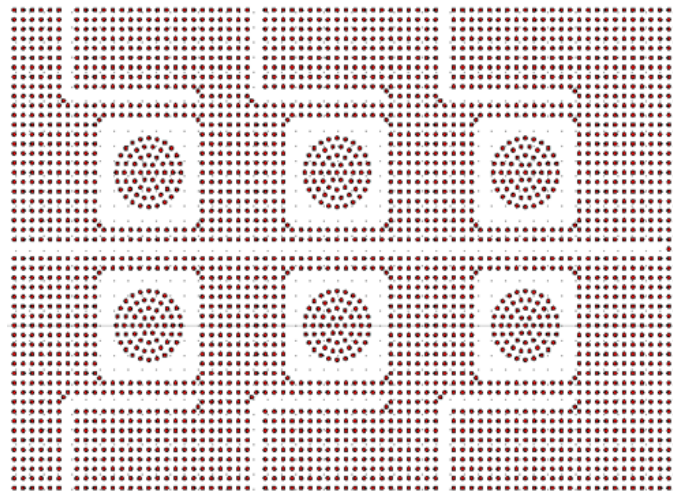


Fig. 3. The final design of the proposed demultiplexer (color online)

We removed 61 dielectric rods in the  $\Gamma$ -M direction to create the input waveguide and then created 6 output waveguides by removing 13 dielectric rods in the M-X direction for each output waveguide. First, we removed a  $9 \times 9$  array of dielectric rods at the appropriate location to create resonant rings between the input waveguide and each output waveguide, then replaced them with a 12-fold pseudo-crystalline structure for each ring. The pseudo-crystal is a 12-fold quasi-periodic structure that consists of a central rod as a core rod, which has 3 orbitals around the radius of the first, second, and third orbitals, respectively,  $r_1$ ,  $r_2$ , and  $r_3$  ( $r = 0.85 \cdot a$ ). The number of dielectric rods in the first, second, and third orbitals is 6, 12, and 12, respectively. This part of the core structure is the resonator ring, so we call it the core structure, for simplicity in the rest of the paper. It has been shown that the resonant wavelength of PhCRRs depends on the refractive index and the geometric dimensions of the core section. Therefore, by choosing different values for these parameters, different resonance wavelengths can be obtained. The sensitivity of the resonance wavelength to the refractive index is very high, and choosing a different refractive index for the core of PhCRRs results in high channel spacing, therefore, the refractive index of the core structure is the same as the main structure in all PhCRRs. The next parameter we can use to control the resonance wavelength is the radius of the dielectric rods in the 12-fold quasi-crystalline structure (12-

sided pattern), we choose the same values for the central rods and the rods in the two inner orbitals in order to have a minimum channel spacing. Each 12-fold quasi-crystalline structure and only different radii are used for the outer orbital rods of each 12-fold quasi-crystalline structure.

### 3. Simulation and results

The most commonly used method to obtain the optical properties of PhC-based devices is finite difference time domain (FDTD). Also, Perfect Matched layer (PML) boundary conditions around our structure were used, the PML width is 500 nm. The grid size ( $\Delta x$  and  $\Delta y$ ) in FDTD parameters is chosen as  $a/18$ , which is equivalent to 40 nm. The time step  $\Delta t$  must satisfy the Chamberlin-Courant rule (hereafter, CCR) due to considerations of simulation stability.  $\Delta t = 0.028$  ns was chosen following the aforementioned rule for the time step. The simulation is performed during 30,000 time steps, which requires 500 minutes of execution time and 32 MB of memory for our proposed demultiplexer. After simulation,  $\lambda_1 = 1555.9$  nm,  $\lambda_2 = 1556.7$  nm,  $\lambda_3 = 1557.8$  nm, and  $\lambda_4 = 1558.9$  nm,  $\lambda_5 = 1559.7$ ,  $\lambda_6 = 1560.8$  nm were obtained for the first, second, third and fourth output channels, respectively. The output spectrum of the demultiplexer is shown in Fig. 4.

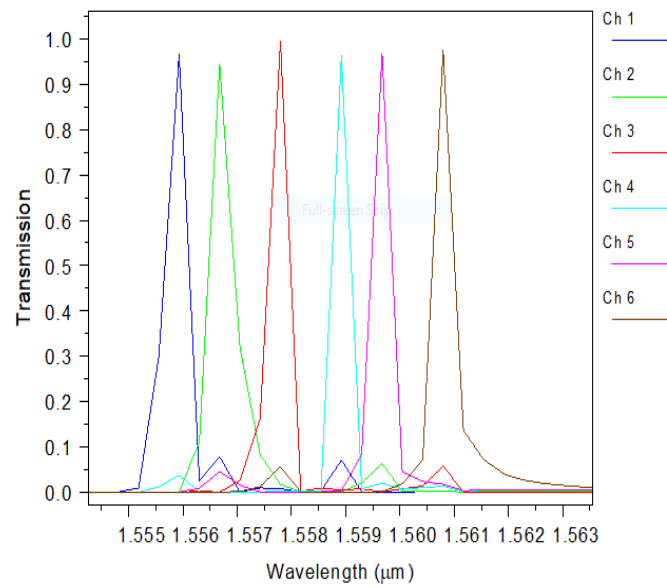


Fig. 4. Output spectrum of the 6-channel demultiplexer on a linear (color online)

The channel spacing is less than 0.98 nm, and the average bandwidth is less than 1.4 nm. The most obvious feature of our structure is its high transmission efficiency, and the channel spacing is small, the minimum transmission

efficiency of the structure is 95% and the overall quality factor ( $Q = \lambda/\Delta\lambda$ ) is more than 4447. The full specifications of the demultiplexer are listed in Table 1, where R is the radius of the outer orbital bars for each channel.

Table 1. Output parameters of demultiplexer

Channel	R(nm)	$\lambda$ (nm)	$\Delta\lambda$ (nm)	Q	Transmission
1	128	1555.9	0.3	5186	96
2	128	1556.7	0.35	4447	95
3	128	1557.8	0.15	10385	100
4	128	1558.9	0.1	15589	96
5	128	1159.7	0.2	7798	97
6	128	1560.8	0.25	6243	97

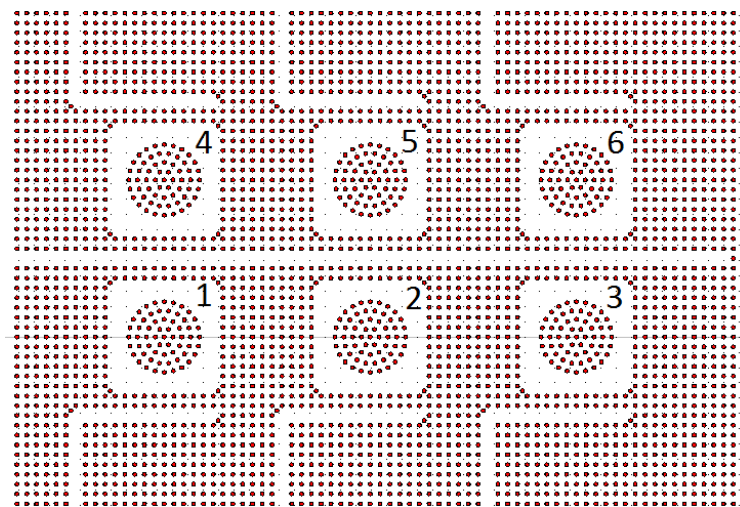


Fig. 5. According to the Fig. 5, ring No. 1, 2, 3, 4, 5, 6 corresponds to the wavelength (color online)

According to Fig. 5, ring No. 1 corresponds to the wavelength of Ch1, ring No. 2 to the wavelength of Ch2, ring No. 3 to the wavelength of Ch3, ring No. 4 to the

wavelength of Ch4, ring No. 5 to the wavelength of Ch5, ring No. 6 to the wavelength of Ch6.

Also, the values of the output spectrum based on dB and interference are listed in Fig. 6 and Table 2, where the interference values are named  $X_{ij}$  ( $i, j$  varies from 1 to 4), which shows the influence of channel  $i$  on channel  $j$  In the central wavelength  $j$  of the channel. The indices  $i$  and  $j$  are shown in the column and row, respectively, in Table 2.

Crosstalk is a very important parameter in the design of optical wavelength demultiplexers. Lower = (better) interference level results in better resolution for output channels. The interference level for our structure varies from -12 dB to -38 dB.

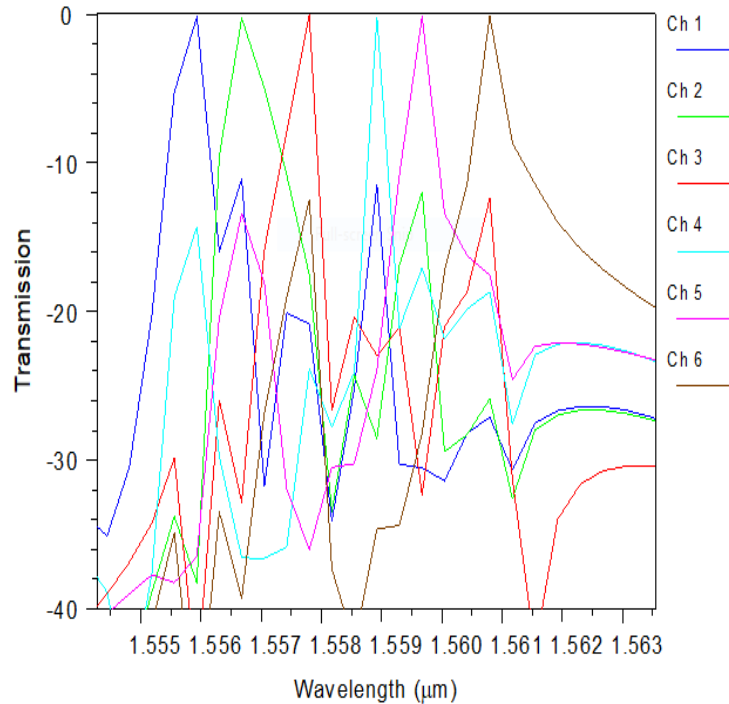


Fig. 6. The output spectrum of the proposed demultiplexer based on the decibel scale (color online)

Table 2. Demultiplexer cross-talk values (dB)

channel	1	2	3	4	5	6
1	-	-	-	-	-	-
2	-	-	-18 dB	-38 dB	-12 dB	-30 dB
3	-22 dB	-16 dB	-	-24 dB	-36 dB	-16 dB
4	-12 dB	-28 dB	-24 dB	-	-24 dB	-34 dB
5	-32 dB	-12 dB	-32 dB	-17 dB	-	-30 dB
6	-28 dB	-26 dB	-13 dB	-20 dB	-18 dB	-

Table 3. Comparison table of previous works in terms of the channel distance parameter

Names of authors	Print year	Channel spacing
Talebzadeh et al. [16]	2017	1.46(6 channel), 1.15 (8 channel)
Talebzadeh et al. [17]	2012	3 nm
Mehdzadehet al. [18]	2016	3.2 nm
Talebzadeh et al. [19]	2016	4.2 nm
Our demultiplexer design		0.98 nm

According to Table 3, in terms of the channel distance parameter, there has been a significant improvement compared to previous similar designs.

#### 4. Conclusion

This study has considered a two-dimensional photonic crystal with an arrangement of silicon circular rods in the airfield, and the PWE method was first used to extract the band structure diagram and RSoft Photonics CAD -Band solve software to extract the photon gap band region using



the related structure. On a silica substrate. By creating linear defects through the removal of rods and changing their radius, the defects created by linear defects in the gaff band area were analyzed and investigated. How to spread and pass the desired wavelengths using RSoft Photonics CAD software. Fullwave software was analyzed using the FDTD simulation method.

Telecommunication wavelength stretching of 1.5559 nm, 1.5567 nm, 1.5578 nm, 1.5589 nm, 1.5597 nm, and 1.5608 nm with an average channel distance of 0.98 nm are well separated with optimization and resonators that are a significant improvement. Compared to previous works [16-19] in terms of  $\lambda$  (nm) and transmission. The performance parameters of the structure were calculated by plane wave expansion and finite difference methods in the time domain, and the throughput gain and the average quality factor related to the designed demultiplexer channels are about 96.83 and 8274.6, respectively.

In this design, we achieved a channel space of 0.98 nm, which is a significant improvement compared to the channel space of previous demultiplexers.

## References

- [1] P. Jiang, C. Ding, X. Hu, Q. Gong, *Phys. Lett. A* **363**, 332 (2007).
- [2] M. L. Shalaev, W. Walasik, T. Sukernik, A. Y. Xu, M. N. Litchinitser, *Nat. Nanotechnology* **14**, 31 (2019).
- [3] P. Rezaee, M. Höft, *Frequency* **71**, 3 (2017).
- [4] A. Andalib, *Photonic Network Communications* **35**, 392 (2018).
- [5] A. Tavousi, *Optik* **179**, 1169 (2019).
- [6] A. Shaverdi, M. Soroosh, E. Namjoo, *International Journal of Optics and Photonics* **12**, 129 (2018).
- [7] S. Robinson, R. Nakkeeran, *Optik* **124**, 3430 (2013).
- [8] Y. H. Ra, R. T. Rashid, X. Liu, J. Lee, Z. Mi, *Advanced Functional Materials* **27**, 1702364 (2017).
- [9] T. Chen, H. Liu, Q. Shen, T. Yue, X. Cao, Z. Ma, *2017 IEEE VCIP* **10**, 1 (2017)
- [10] J. Park, C. Baik, F. Lee, *Optics Express* **15**, 1461 (2007).
- [11] H. Alipour-Banaei, F. Mehdizadeh, M. Hassangholizadeh-Kashtiban, *Optik* **124**, 4416 (2013).
- [12] B. Momeni, J. Huang, M. Soltani, M. Askari, S. Mohammadi, M. Rakhshandehroo, A. Adibi, *Optics Express* **14**, 2413 (2006).
- [13] F. Cheraghi, M. Soroosh, G. Akbarizadeh, *Superlattices and Microstructures* **113**, 359 (2018).
- [14] F. Mehdizadeh, M. Soroosh, H. Alipour-Banaei, E. Farshidi, *ELECO 446-450*, (2017).
- [15] R. Goyal, B. K. Nayak, A. Tulapurkar, V. G. Achanta, *Front. Phys.* **6**, 152 (2019).
- [16] E. Talebzadeh, M. Soroosh, Y. S. Kaviani, F. Mehdizadeh, *Photonic Network Communications* **34**, 248 (2017).
- [17] R. Talebzadeh, M. Soroosh, T. Daghooghi, *IETE Journal of Research* **62**(6), 866 (2016).
- [18] F. Mehdizadeh, M. Soroosh, *Photonic Network Communications* **31**, 65 (2016).
- [19] R. Talebzadeh, M. Soroosh, Y. S. Kaviani, F. Mehdizadeh, *Optik* **140**, 331 (2017).
- [20] A. Yariv, *Quantum Electronics*, 3rd ed, Wiley, (1989).
- [21] W. Bogaerts, P. de Heyn, T. van Vaerenbergh, K. de Vos, S. Kumar Selvaraja, T. Claes, P. Dumon, P. Bienstman, D. van Thourhout, R. Baets, *Laser and Photonics Reviews* **6**, 47 (2012).

\*Corresponding author: S.masoumi.ee@gmail.com